Modeling spin dynamics with tuned and matched probes

Soumyajit Mandal (sxm833@case.edu)

Transmit phase

The relationship between i) the output open-circuit voltage provided by the transmitter (denoted by V_s), and ii) the coil current (I_c) that sets the RF magnetic field (B_1), can be modeled with reference to the circuit diagram shown in Figure 1. The coil is modeled using an inductance L in series with a resistance R_c, while the transmitter is modeled by the voltage source V_s in series with a resistance R_s (typically 50 Ω). This circuit must be simulated in the time domain since the spin dynamics controlled by B_1 are nonlinear.

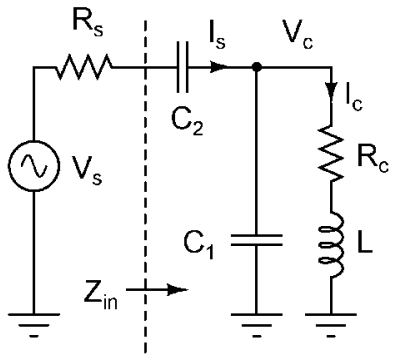

Figure 1: *Circuit model of a tuned and matched NMR probe during transmission.*

Design of the matching network: The capacitors C_1 and C_2 are chosen in order to provide impedance matching for maximum power transfer, i.e., such that the input impedance Z_{in} seen "looking in" to the probe is equal to R_s at the operating frequency of interest (denoted by $\omega_0 = 2\pi f_0$). In practice, the value of the shunt capacitor C_1 is adjusted in order to absorb the parasitic capacitance of the coil. Note that while other capacitive matching circuits are possible, this "shunt tuned, series matched" design works well for a wide range of coils and is thus the most common design. However, very small, low-Q coils, or very large, high-Q coils cannot be effectively impedance-matched using this circuit. In the latter case, a "series tuned, shunt matched" circuit (i.e., an input-output reversed version of the circuit shown above) is often used instead.

The frequency-dependent input impedance of the probe is given by

$$\begin{aligned} Z_{in}(\omega) &= \frac{1}{j\omega C_2} + \frac{\left(j\omega L + R_c\right)\frac{1}{j\omega C_1}}{j\omega L + R_c + \frac{1}{j\omega C_1}} \\ &= \frac{-j}{\omega C_2} + \frac{j\omega L + R_c}{\underbrace{\left(1-\omega^2 L C_1\right) + j\omega R_c C_1}_{Z_1}}. \end{aligned}$$

This complex equation can be decomposed into two independent equations for the real and imaginary components of Z_{in}. The desired values of these components are

$$\mathrm{Re}\left(Z_{in}\left(\omega_0\right)\right) = R_s = 50\,\Omega, \quad \text{and}$$
$$\mathrm{Im}\left(Z_{in}\left(\omega_0\right)\right) = \frac{-1}{\omega C_2} + \mathrm{Im}\left(Z_1\left(\omega_0\right)\right) = 0.$$

Thus, we have two nonlinear equations in two unknowns (C_1 and C_2). These can be solved using a standard gradient-based numerical optimizer that minimizes the net squared impedance error given by

$$f_{err}\left(C_1, C_2\right) = \left[\mathrm{Re}\left(Z_{in}\left(\omega_0\right)\right) - R_s\right]^2 + \left[\mathrm{Im}\left(Z_{in}\left(\omega_0\right)\right)\right]^2.$$

Consider a typical situation in which we need to match a coil with L = 500 nH and R_c = 1 Ω to R_s = 50 Ω at f_0 = 8 MHz; the resulting coil Q = 25. The optimizer (written in MATLAB) predicts the values C_1 = 680 pF and C_2 = 113 pF. Figure 2 confirms that these values do satisfy both matching conditions at the desired operating frequency.

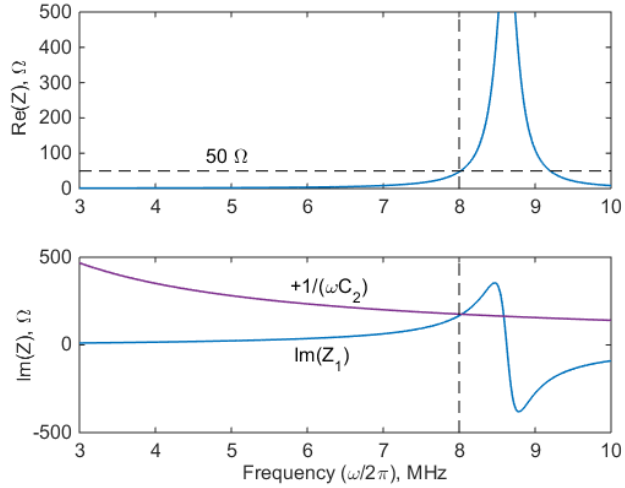

Figure 2: *Real and imaginary parts of the input impedance of the probe versus frequency.*

Solving for the coil current: Once the capacitance values have been calculated, we can use simple circuit analysis (Kirchoff's current and voltage laws) to find the relationship between V_s and I_c. It is convenient to do this in the Laplace (i.e., complex frequency) domain. The relevant equations are

$$V_c = (sL + R_c)I_c,$$
$$I_s = sC_1V_c + I_c, \quad \text{and}$$
$$V_c = V_s - I_sR_s - \frac{I_s}{sC_2}.$$

Here V_c is the coil voltage, while I_s is the current being supplied by the source. We can eliminate these intermediate variables after some algebra, thus resulting in a single equation that connects V_s to I_c:

$$\frac{sC_2V_s}{I_c} = s^3C_1C_2R_sL + s^2\left(L(C_1 + C_2) + C_1C_2R_sR_c\right) + s\left((C_1 + C_2)R_c + C_2R_s\right) + 1.$$

In order to simplify this expression, we define a normalized (dimensionless) time variable $\tau = \omega_p t$, where $\omega_p = \sqrt{LC_1}$. The corresponding normalized Laplace transform variable is $s_n = s/\omega_p$, resulting in

$$\frac{s_n C_2}{\sqrt{LC_1}}\frac{V_s}{I_c} = {s_n}^3\frac{C_1C_2R_sL}{\left(LC_1\right)^{3/2}} + {s_n}^2\frac{\left(L(C_1+C_2)+C_1C_2R_sR_c\right)}{LC_1} + s\frac{\left((C_1+C_2)R_c+C_2R_s\right)}{\sqrt{LC_1}} + 1.$$

Next, we define the dimensionless variable $n = C_1/C_2$ (generally *n* = 4-10), which results in

$$\frac{s_n C_1}{n\sqrt{LC_1}}\frac{V_s}{I_c} = {s_n}^3\frac{{C_1}^2R_sL}{n\left(LC_1\right)^{3/2}} + {s_n}^2\frac{\left(LC_1(n+1)+{C_1}^2R_sR_c\right)}{nLC_1} + s_n\frac{\left(C_1(n+1)R_c+C_1R_s\right)}{n\sqrt{LC_1}} + 1,$$

$$\frac{s_n}{n}\sqrt{\frac{C_1}{L}}\frac{V_s}{I_c} = \frac{{s_n}^3}{n}\sqrt{\frac{C_1}{L}}R_s + \frac{{s_n}^2}{n}\left((n+1)+\frac{C_1}{L}R_sR_c\right) + \frac{s_n}{n}\sqrt{\frac{C_1}{L}}\left((n+1)R_c+R_s\right).$$

After this, we define the characteristic impedance of the probe to be $Z_0 = \sqrt{L/C_1}$; this variable has dimensions of Ohms. The equation now simplifies to

$$\frac{s_n}{nZ_0}\frac{V_s}{I_c} = \frac{{s_n}^3}{nZ_0}R_s + \frac{{s_n}^2}{n}\left((n+1)+\frac{R_sR_c}{Z_0^2}\right) + \frac{s_n}{nZ_0}\left((n+1)R_c+R_s\right),$$

$${s_n}^3 + {s_n}^2\left((n+1)\frac{Z_0}{R_s}+\frac{R_c}{Z_0}\right) + s_n\left((n+1)\frac{R_c}{R_s}+1\right) + \frac{nZ_0}{R_s} = \frac{s_n}{R_s}\frac{V_s}{I_c}.$$

We can now directly write the corresponding differential equation in the normalized time domain by remembering that $\mathcal{L}\left(f'(t)\right) = sF(s) - f(0)$ where $\mathcal{L}(\cdot)$ denotes the Laplace transform. Thus, assuming zero initial conditions, we can simply make the transformation $s_n \leftrightarrow d/d\tau$ to get

$$\frac{d^3I_c}{d\tau^3} + c_3\frac{d^2I_c}{d\tau^2} + c_2\frac{dI_c}{d\tau} + c_1I_c = \frac{1}{R_s}\frac{dV_s}{dt}, \quad \text{where}$$

$$c_3 = \left((n+1)\frac{Z_0}{R_s}+\frac{R_c}{Z_0}\right), \quad c_2 = \left((n+1)\frac{R_c}{R_s}+1\right), \quad c_1 = \frac{nZ_0}{R_s}.$$

This is a simple third-order ordinary differential equation (ODE) with constant coefficients that can be readily solved using standard ODE solvers. It can be further simplified by normalizing the coil current I_c to its ideal value I_{c0} for a perfectly-matched probe in steady-state. The latter can be derived by using an energy conservation argument. For perfect matching, the input impedance of the probe is equal to R_s, so the source current is $I_{s0} = V_{s0}/\left(R_s + Z_{in}\right) = V_{s0}/(2R_s)$ where V_{s0} is the amplitude of the source voltage. Thus, the power delivered by the source is $P_s = I_{s0}^2R_s/2 = V_{s0}^2/(8R_s)$. The same power must be dissipated in the coil's series resistance R_c, so

$$P_s = \frac{V_{s0}^2}{8R_s} = P_c = \frac{{I_{c0}}^2 R_c}{2}$$

$$\Rightarrow I_{c0} = \frac{V_{s0s}}{2\sqrt{R_c R_s}}.$$

Let us define the normalized coil current $I_{cn} = I_c / I_{c0}$. In terms of this dimensionless quantity, we get

$$\frac{d^3 I_{cn}}{d\tau^3} + c_3 \frac{d^2 I_{cn}}{d\tau^2} + c_2 \frac{dI_{cn}}{d\tau} + c_1 I_{cn} = \frac{1}{I_{c0} R_s} \frac{dV_s}{dt} = \frac{2}{V_{s0}} \sqrt{\frac{R_c}{R_s}} \frac{dV_s}{dt}.$$

In practice, we are interested in complex exponential inputs $V_s = V_{s0} e^{j(\omega_0 t + \phi)}$ where ω_0 is the RF frequency and ϕ is the phase of the pulse in the rotating frame. In terms of the normalized time variable, the inputs are given by $V_s = V_{s0} e^{j(\omega_n \tau + \phi)}$ where $\omega_n = \omega_0 / \omega_p$ is the normalized RF frequency. Thus, the right-hand side of the ODE becomes

$$\frac{d^3 I_{cn}}{d\tau^3} + c_3 \frac{d^2 I_{cn}}{d\tau^2} + c_2 \frac{dI_{cn}}{d\tau} + c_1 I_{cn} = 2j\omega_n \sqrt{\frac{R_c}{R_s}} e^{j(\omega_n \tau + \phi)},$$

$$\Rightarrow \frac{d^3 I_{cn}}{d\tau^3} + c_3 \frac{d^2 I_{cn}}{d\tau^2} + c_2 \frac{dI_{cn}}{d\tau} + c_1 I_{cn} = 2\omega_n \sqrt{\frac{R_c}{R_s}} \left(-\sin(\omega_n \tau + \phi) + j \cos(\omega_n \tau + \phi) \right).$$

We can solve this complex ODE by separately considering the real and imaginary input components (which are proportional to $-\sin(\omega_n \tau)$ and $\cos(\omega_n \tau)$, respectively), and then adding the results. In particular, if the solutions to the real and imaginary input components are $I_{c,re}$ and $I_{c,im}$, respectively, then the complex solution is $I_{cn}(\tau) = I_{c,re}(\tau) + jI_{c,im}(\tau)$.

Conversion to the rotating frame: The analysis above has ignored the effect of the absolute phase ψ of the RF waveform. If its effects need to be considered (e.g. for very short RF pulses), the input waveform for the ODE should be written as $V_s = V_{s0} e^{j(\omega_n \tau + \phi + \psi)}$. The resulting complex coil current should be converted to the rotating frame as follows:

$$I_{cr}(\tau) = I_{cn}(\tau) e^{-j(\omega_n \tau + \psi)} .$$

This solution process largely eliminates the counter-rotating component of the coil current. Any residual counter-rotating current has a frequency of $2\omega_n$ and can be removed by averaging $I_{cr}(\tau)$ over time windows of length $\tau_w = 1/(2\omega_n)$. The resulting discrete-time sequence $I_{cr}(n)$ can now be easily converted into real time $t = \tau / \omega_p$ and fed into existing spin dynamics simulation code.

Effects of discontinuities: An issue with our analysis is the fact that in practice the input voltage waveform $V_s(\tau)$ has discontinuities, in particular at the start and end of each RF pulse. Additional discontinuities can also occur within composite RF pulses due to amplitude and phase modulation. The derivative $dV_s/d\tau$ for

the real part of the input waveform at such discontinuities has an additional term proportional to the size of the jump that is given by

$$\delta(\tau-\tau_i)\left[A_i\sin(\omega_n\tau+\phi_i+\psi)-A_{i+1}\sin(\omega_n\tau+\phi_{i+1}+\psi)\right],$$

where τ_i is the instant at which the discontinuity occurs, (A_i, ϕ_i) and (A_{i+1}, ϕ_{i+1}) are the pulse amplitudes and phases before and after the discontinuity, respectively, and $\delta(t)$ is the Dirac delta function. A similar term occurs for the imaginary part of the input waveform, but with sin replaced by cos. The response of the coil current to each perturbation of this type is simply a scaled version of the impulse response $h(\tau)$ of the linear system

$$TF(s_n)=\frac{I_{cn}(s_n)}{s_nV_s(s_n)}=2\sqrt{\frac{R_c}{R_s}}\left(\frac{1}{s_n^3+c_3s_n^2+c_2s_n+c_1}\right).$$

In order to obtain the normalized coil current I_{cn} accurately, these impulse responses (which are sinusoidal oscillations with decaying exponential envelopes) should be added to the solution of the ODE before it is converted to the rotating frame.

Example: In a typical scenario, we vary the input amplitude V_{s0} in the sequence $a(n)$ = [0, k, 0] in order to simulate a simple rectangular RF pulse of amplitude k. The differential equation is then solved with zero initial conditions for the first non-zero segment in $a(n)$ (in this case, the second segment). Note that using zero initial conditions amount to assuming that the coil current has completely decayed following the previous RF pulse, which is usually a good assumption. Finally, the same differential equation is solved for all later segments $a(n)$, but with initial conditions that correspond to the final instant of the previous segment. This procedure ensures that the solution remains continuous.

Consider an example in which we seek to match a coil with L = 10 µH and Q = 50 to R_s = 50 Ω at f_0 = 1 MHz. The predicted matching capacitor values are C_1 = 2.13 nF and C_2 = 405 pF, resulting in n = 5.27. Figure 3 shows the simulated RF and rotating frame waveforms for a rectangular input pulse with normalized amplitude k = 1 and duration t_p = 25 µs. The rise and fall time effects associated with limited probe bandwidth are clearly visible. Also, in this case the discontinuities in $dV_s(\tau)/d\tau$ that are present at the beginning and end of the pulse have little effect on the coil current in the rotating frame.

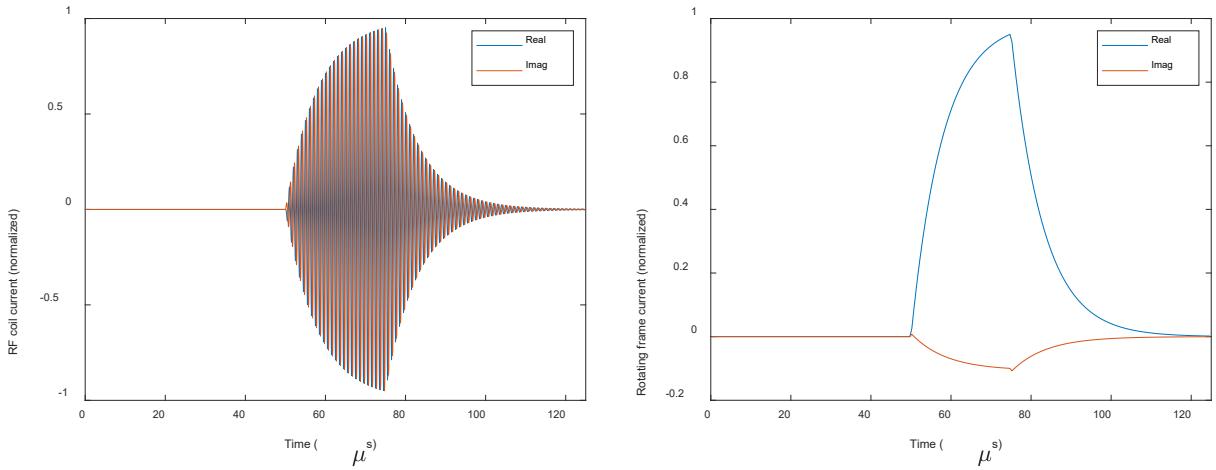

Figure 3: *Simulated pulse shape for t_p = 25 µs: RF waveform (left) and rotating frame waveform (right).*

Figure 4 shows the output of the same matched probe for a longer pulse (t_p = 50 µs). In this case, there is enough time for the pulse amplitude to settle to nearly its final steady-state value of k = 1.

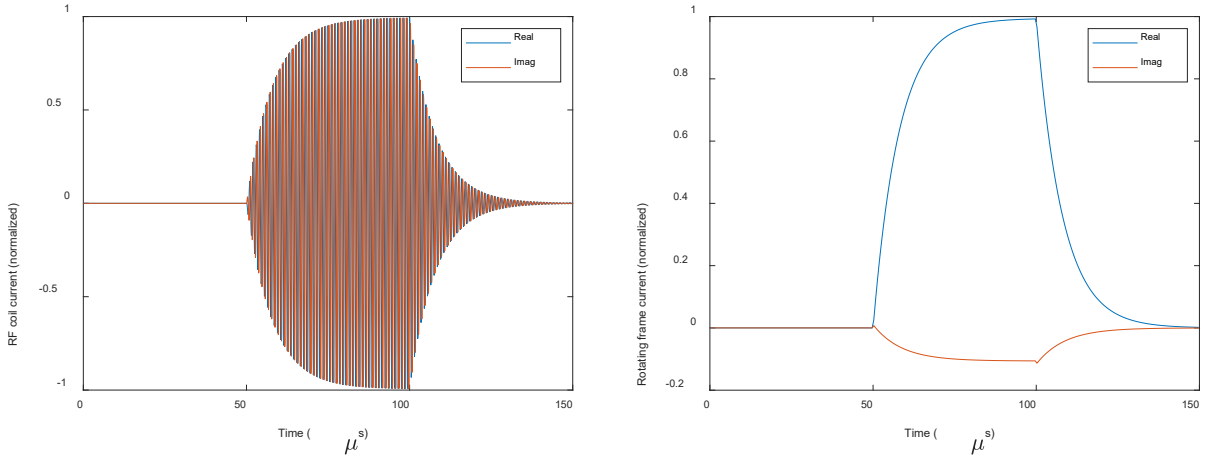

Figure 4: *Simulated pulse shape for t_p = 50 µs: RF waveform (left) and rotating frame waveform (right).*

Receive phase

The relationship between i) the coil voltage V_{in} induced by the precessing nuclear spins, and ii) the output voltage V_{out} measured by the receiver, can be modeled with reference to the circuit diagram shown in Figure 5. Here we have assumed that the input impedance of the receiver is identical to the output impedance R_s of the transmitter, as is often the case. It is sufficient to simulate this circuit in the frequency domain since both the matching network and the receiver electronics can be assumed to be linear.

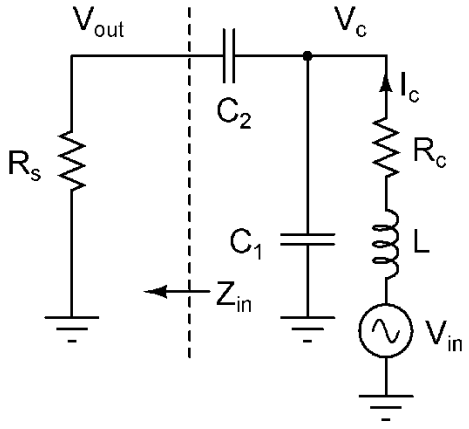

Figure 5: *Circuit model of a tuned and matched NMR probe during reception.*

Solving for the received voltage: The transfer function of this network from V_{in} to V_c (the voltage across the coil) in the s-domain can be easily found by treating it as a voltage divider. The result is

$$\frac{V_c}{V_{in}} = \frac{\left(\frac{1}{sC_1} \| \left(R_s + \frac{1}{sC_2}\right)\right)}{sL + R_c + \left(\frac{1}{sC_1} \| \left(R_s + \frac{1}{sC_2}\right)\right)} = \frac{\frac{n + sC_1R_s}{(n+1) + sC_1R_s}}{s^2LC_1 + sC_1R_c + \frac{n + sC_1R_s}{(n+1) + sC_1R_s}}.$$

A simpler voltage divider can now be used to model the relationship between V_c and V_{out}, resulting in an overall transfer function of

$$\frac{V_{out}}{V_{in}} = \frac{V_c}{V_{in}} \frac{R_s}{R_s + \frac{1}{sC_2}} = \frac{V_c}{V_{in}} \frac{sC_1R_s}{n + sC_1R_s} = \frac{sC_1R_s}{n + sC_1R_s} \frac{\frac{n + sC_1R_s}{(n+1) + sC_1R_s}}{s^2LC_1 + sC_1R_c + \frac{n + sC_1R_s}{(n+1) + sC_1R_s}}$$

$$= \frac{\frac{sC_1R_s}{(n+1) + sC_1R_s}}{s^2LC_1 + sC_1R_c + \frac{n + sC_1R_s}{(n+1) + sC_1R_s}} = \frac{sC_1R_s}{\left[sC_1R_s + (n+1)\right]\left[s^2LC_1 + sC_1R_c\right] + sC_1R_s + n}.$$

The corresponding normalized Laplace transform variable is $s_n = s / \omega_p = s\sqrt{LC_1}$, resulting in

$$\frac{V_{out}}{V_{in}} = \frac{\frac{s_n}{\sqrt{LC_1}} C_1R_s}{\left[\frac{s_n}{\sqrt{LC_1}} C_1R_s + (n+1)\right]\left[\frac{s_n^2}{LC_1} LC_1 + \frac{s_n}{\sqrt{LC_1}} C_1R_c\right] + \frac{s_n}{\sqrt{LC_1}} C_1R_s + n}$$

$$= \frac{s_n \frac{R_s}{Z_0}}{\left[s_n \frac{R_s}{Z_0} + (n+1)\right]\left[s_n^2 + s_n \frac{R_c}{Z_0}\right] + s_n \frac{R_s}{Z_0} + n} = \frac{s_n}{s_n^3 + s_n^2\left(\frac{(n+1)Z_0}{R_s} + \frac{R_c}{Z_0}\right) + s_n\left(1 + (n+1)\frac{R_c}{R_s}\right) + \frac{nZ_0}{R_s}}.$$

Using the same definitions as for the transmitter, i.e.,

$$c_3 = \left((n+1)\frac{Z_0}{R_s} + \frac{R_c}{Z_0}\right), \quad c_2 = \left((n+1)\frac{R_c}{R_s} + 1\right), \quad c_1 = \frac{nZ_0}{R_s}$$

we finally get the transfer function of the network:

$$TF(s) = \frac{V_{out}}{V_{in}} = \frac{s_n}{s_n^3 + c_3s_n^2 + c_2s_n + c_1}.$$

The peak magnitude (i.e., voltage gain) of *TF* is easy to estimate using an energy conservation argument. Assuming perfect matching and lossless components, the *LC* network shown in Figure 5 transforms its terminal impedance from R_c to R_s without dissipating energy. Thus, the transformed open circuit voltage

must satisfy $(V_{in}')^2 / 2R_s = (V_{in})^2 / 2R_c$, such that $V_{in}' / V_{in} = \sqrt{R_s / R_c}$. Half of this voltage appears across the receiver, so we get

$$TF_1(\omega)\big|_{max} = \frac{V_{out}}{V_{in}} = \frac{1}{2}\left(\frac{V_{in}'}{V_{in}}\right) = \frac{1}{2}\sqrt{\frac{R_s}{R_c}}.$$

It is also interesting to compare the expression for receiver TF with the transfer function in transmit mode. Using our earlier results, we find that

$$\frac{I_c}{V_s / R_s} = \frac{s_n}{s_n^3 + c_3 s_n^{\,2} + c_2 s_n + c_1}.$$

Thus, the voltage-mode transfer function $TF_1(\omega) = V_{out} / V_{in}$ in receive mode is identical to the current-mode transfer function $I_c / \left(V_s / R_s\right)$ in transmit mode. This is a consequence of the fact that the *LC* network (excluding the terminal resistances R_c and R_s) is passive and lossless and thus conserves energy. As a result, $V_{in} I_{in} = V_{out} I_{out}$ and $V_{out} / V_{in} = I_{in} / I_{out}$, i.e., the circuit behaves as an ideal transformer. This explains why we get the same transfer function when we reverse the input and output ports and replace voltage with current.

It is interesting to note that $TF_1(\omega)$ also defines how thermal noise generated by the coil resistance R_c is filtered by the probe before reaching the receiver. Such filtered noise ultimately limits the precision of the measurement. Specifically, the power spectrum density (PSD) of receiver noise is given by

$$\overline{v_{ni}^2} = 4kTR_c \left|TF_1(\omega)\right|^2.$$

Another effect to consider is the fact that the NMR voltage waveform V_{in} is detected using Faraday induction, i.e., $V_{in}(t) = d\phi / dt$ where $\phi = \int \mathbf{B} \cdot dS$ is the magnetic flux generated by the precessing spins within the receive coil. In the s-domain, we can write this relationship as $V_{in}(s) = sS_{rx}M(s)$ where S_{rx} is the coil sensitivity function in receive mode and $M(s)$ is the magnetization vector estimated by the spin dynamics code. Moreover, $M(\omega)$ also increases linearly with Larmor frequency due to Boltzmann statistics; this effect is generally not included in spin dynamics simulations, but we can model it by including another factor of ω_n in the transfer function. Since S_{rx} is a constant for a given coil and sample geometry, the modified transfer function can now be written as

$$TF_2(s) = \frac{V_{out}(s)}{M(s)} = -jS_{rx}\frac{s_n^3}{s_n^3 + c_3 s_n^2 + c_2 s_n + c_1}.$$

In terms of the distribution of the B_0 field, we can further write $s_n = j\omega_n = j\left(\omega_0 / \omega_p\right) = j\gamma B_0 / \omega_p$ where ω_0 and B_0 are the local Larmor frequency and B_0 field magnitude, respectively.

Example: Figure 6 shows the estimated receiver transfer functions V_{out}/V_{in} and V_{out}/M for the same probe parameters assumed in the earlier section. The band-pass nature of these functions limits the bandwidth of the NMR signals that can be received by the system.

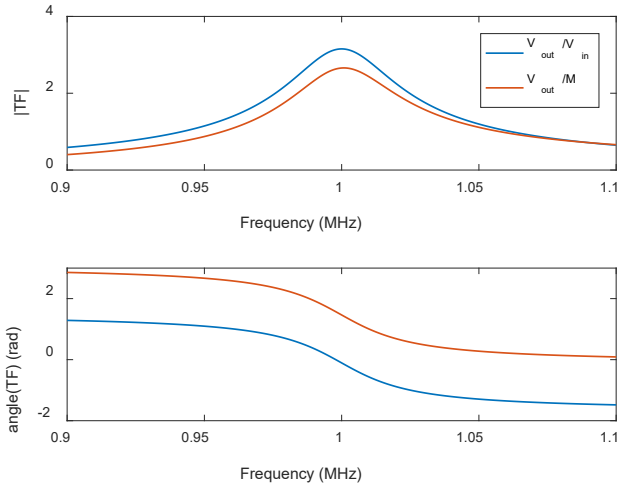

Figure 6: *Estimated receiver transfer functions for the same probe considered in the earlier section.*

Simulation results

In order to study the effects of limited probe bandwidth, we first study the asymptotic magnetization and spin echoes generated by an "ideal" Carr-Purcell-Meiboom-Gill (CPMG) pulse sequence in a uniform B_0 gradient (by "ideal", we mean that probe bandwidth effects can be ignored). Figure 7 summarizes the simulation results, which are in agreement with published work. Note that the x-axis in Figure 7(a)-(b) is in units of the normalized offset frequency, i.e., $\Delta\omega_0 = \left(\omega_{RF} - \gamma\left|\mathbf{B}_0\right|\right)/\omega_{1c}$ where ω_{RF} is the excitation frequency (assumed to be equal to both the average Larmor frequency and the probe tuning frequency) and ω_{1c} is the nutation frequency (assumed to be uniform across the sample). The latter is defined as $\omega_{1c} = \gamma B_{1c}$, where B_{1c} is the magnitude of the circularly polarized component of the RF magnetic field that is orthogonal to $\mathbf{B}_0$.

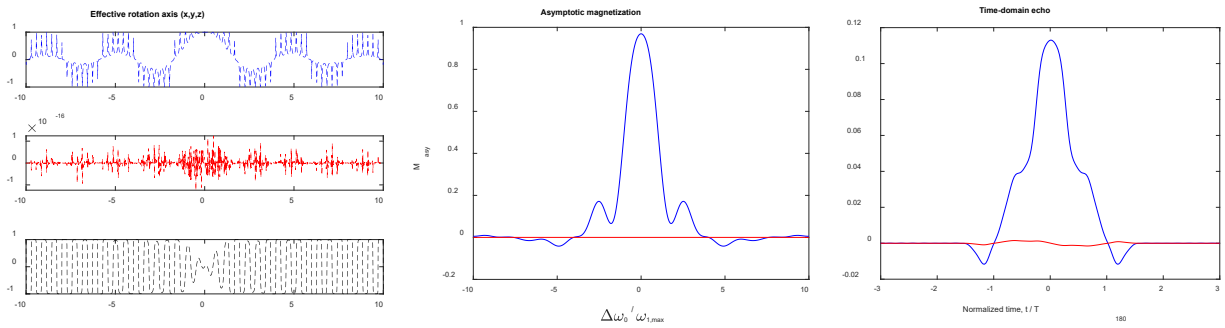

Figure 7: *CPMG pulse sequence in a uniform B_0 field gradient, with probe bandwidth effects ignored: (a) Effective rotation axis as a function of the normalized offset frequency $\Delta\omega_0$; (b) asymptotic magnetization; (c) asymptotic echo. The following pulse sequence parameters were assumed: $T_{180} = 2T_{90}$, acquisition time $T_{acq} = 3T_{180}$. For (b)-(c), blue and red lines denote the real and complex parts of the complex signal, respectively.*

The simulation is then repeated for the same tuned probe assumed in earlier sections (L = 10 µH, Q = 50, R_s = 50 Ω, and f_0 = 1 MHz) for excitation and refocusing pulse lengths of T_{90} = 25 µs and T_{180} = 50 µs, respectively. The results are shown in Figure 8. Some of the noteworthy effects of the limited probe bandwidth include i) significant rise and fall times for the excitation and refocusing pulses; ii) reduced

refocusing bandwidth; and iii) low-pass filtering of the echo waveform. Also, notice the nearly 90° phase shift in the received echo as compared to that in Figure 7: this is due to the use of inductive detection (i.e., the fact that $V_{in}(t) = d\phi / dt$).

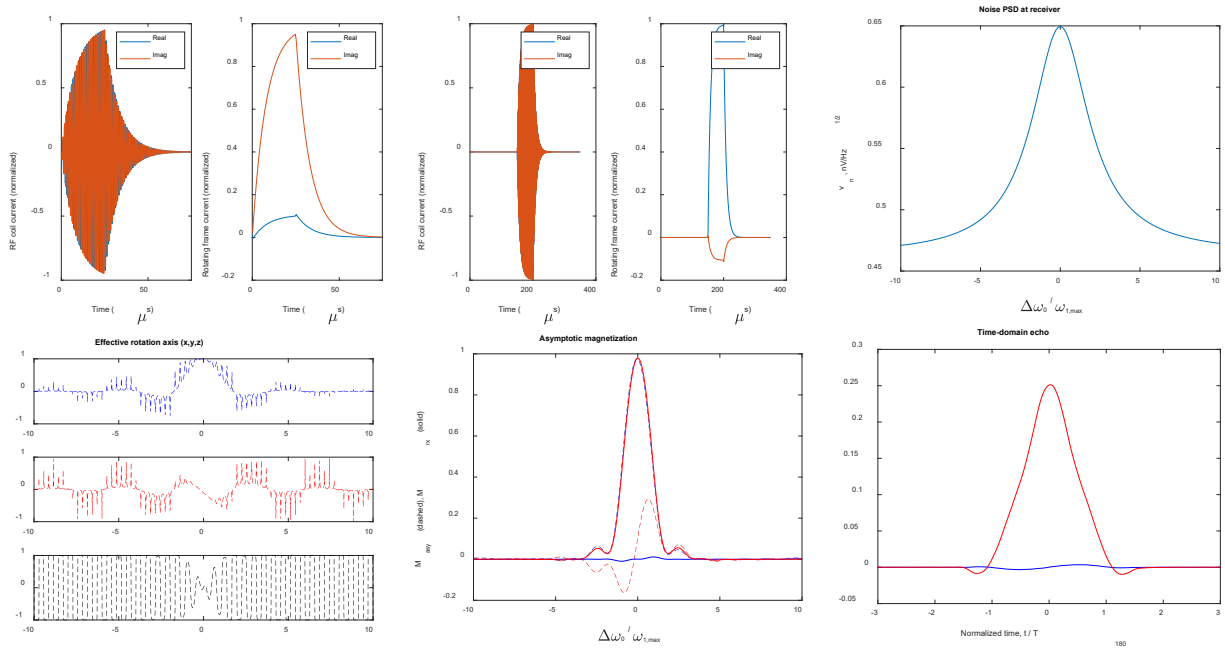

Figure 8: *CPMG pulse sequence in a uniform B_0 field gradient, with probe bandwidth effects included: (a) Excitation pulse in the laboratory and rotating frames; (b) refocusing cycle in the laboratory and rotating frames; (c) noise power spectral density (PSD) at the receiver input terminal, assuming a noise figure (NF) of 1 dB; (d) effective rotation axis as a function of the normalized offset frequency $\Delta\omega_0$; (e) asymptotic magnetization before and after the receiver; (f) asymptotic echo. The following probe and pulse sequence parameters were used: L = 10 µH, Q = 50, R_s = 50 Ω, f_0 = 1 MHz, T_{90} = 25 µs, $T_{180} = 2T_{90}$, $T_{acq} = 3T_{180}$. For (a), (b), (e), and (f), blue and red lines denote the real and complex parts of the complex signal, respectively.*

Appendix: MATLAB simulation code

All simulation code was written in MATLAB. Here we present some commented examples to illustrate how the code can be used.

Spin dynamics only, no probe bandwidth effects

```
[sp, pp] = set_params_matched; % Define system parameters
[masy,echo_asy,tvect]=calc_masy_ideal(sp,pp); % Simulate ideal system
```

Including finite probe bandwidth

```
[sp, pp] = set_params_matched; % Define system parameters
[mrx,echo_rx,tvect,SNR]=calc_masy_matched_probe(sp,pp); % Simulate narrowband system
```

Effects of varying probe bandwidth

In this example, we study the effect of changing the coil *Q,* which is inversely proportional to the probe bandwidth. The MATLAB script is reproduced below:

```
[sp, pp] = set_params_matched; % Define system parameters

Qvec = linspace(10,100,11); % Vary coil Q
```

```
SNR = zeros(1, length(Qvec)); % Storage for output variables
echo_rx = zeros(4*length(sp.del_w),length(Qvec));
mrx = zeros(length(Qvec),length(sp.del_w));

% Run simulations
for i=1:length(Qvec)
    % Turn plotting off to reduce the number of plots
    sp.plt_mn=0; sp.plt_tx=0; sp.plt_rx=0; sp.plt_axis=0; sp.plt_echo=0;
    sp.Q = Qvec(i); % Change coil Q

    % Simulate narrowband system
    [mrx(i,:),echo_rx(:,i),tvect,SNR(i)]=calc_masy_matched_probe(sp,pp);
end

% Plot results
figure; imagesc(sp.del_w,Qvec,abs(mrx)); % Asymptotic magnetization
figure; imagesc(tvect/pi,Qvec,abs(echo_rx)'); % Time-domain echo magnetization
figure; plot(Qvec,SNR); % SNR
```

Simulation results generated by this script are shown in Figure 9 as a function of coil Q. The figure shows that the bandwidth of the magnetization in the offset frequency domain decreases as Q increases, since the probe becomes more narrow-band. Conversely, the width of the time-domain echo increases with Q, as expected. Finally, the signal-to-noise ratio (SNR) of the measurement increases roughly as $Q^{1/2}$ in voltage units. This is because the coil resistance decreases as $1/Q$, resulting in a noise PSD that also decreases as $1/Q$ (in power units) or $1/Q^{1/2}$ (in voltage units). Note that SNR has been calculated assuming that the optimum matched filter (for colored noise) is being used.

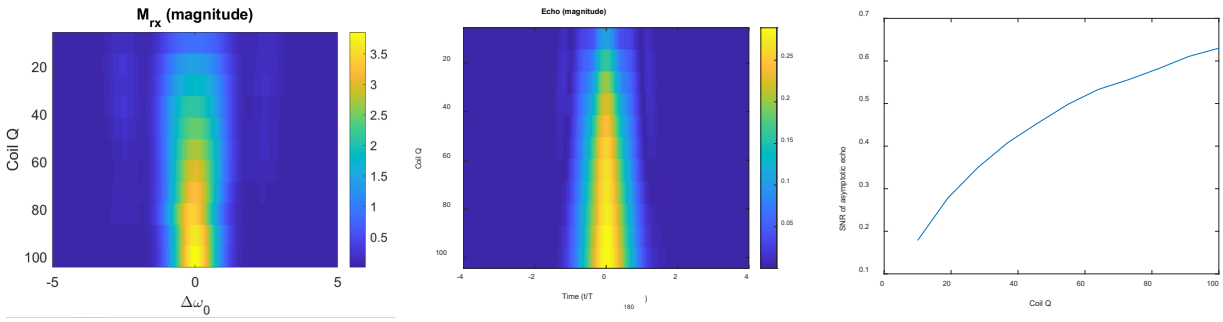

Figure 9: *CPMG pulse sequence in a uniform B_0 field gradient, with probe bandwidth effects included, as a function of coil Q: (a) Asymptotic magnetization; (b) asymptotic echo; (c) signal-to-noise ratio (SNR) in voltage units. The following probe and pulse sequence parameters were used: L = 10 µH, Q = [10-100], R_s = 50 Ω, f_0 = 1 MHz, T_{90} = 25 µs, $T_{180} = 2T_{90}$, $T_{acq} = 3T_{180}$.*

Effects of probe tuning error

Here we study the effects of probe tuning error, i.e., non-zero offset Δf between i) the input RF frequency, and ii) the frequency at which the probe is impedance-matched. The MATLAB script is reproduced below:

```
[sp, pp] = set_params_matched; % Define system parameters

% Vary matching frequency (in units of probe BW = fin/Q)
fin = sp.fin; Q = sp.Q;
f0_vec = fin+(fin/Q)*linspace(-5,5,21);

SNR = zeros(1, length(f0_vec)); % Storage for output variables
echo_rx = zeros(4*length(sp.del_w),length(f0_vec));
mrx = zeros(length(f0_vec),length(sp.del_w));

% Run simulations
for i=1:length(f0_vec)
```

```
    % Turn plotting off to reduce the number of plots
    sp.plt_mn=0; sp.plt_tx=0; sp.plt_rx=0; sp.plt_axis=0; sp.plt_echo=0;
    sp.f0 = f0_vec(i); % Change coil Q

    % Simulate narrowband system
    [mrx(i,:),echo_rx(:,i),tvect,SNR(i)]=calc_masy_matched_probe(sp,pp);
end

% Plot results
figure; imagesc(sp.del_w,(f0_vec-f0)/(fin/Q),abs(mrx)); % Asymptotic magnetization
figure; imagesc(tvect/pi, (f0_vec-f0)/(fin/Q),abs(echo_rx)'); % Time-domain echo
figure; plot((f0_vec-f0)/(fin/Q),SNR); % SNR
```

Here we assume that Δf (normalized to the nominal probe bandwidth of f_0/Q) varies over the [−5, 5] range. Simulation results generated by the script are shown in Figure 10. Figure 10(a) shows that the envelopes of the RF pulses are distorted from the exponential functions that occur for properly-tuned probes (i.e., when $\Delta f = 0$). Figure 10(b) shows the SNR of the asymptotic echo after matched filtering. As expected, the SNR is approximately constant within the probe bandwidth, i.e., for $|\Delta f| \leq 0.5$. Beyond this range, the SNR quickly decreases. Figure 10(c)-(d) show the asymptotic echo in the frequency and time domains, respectively. The effects of filtering by the mis-tuned receiver are clearly visible in the frequency domain.

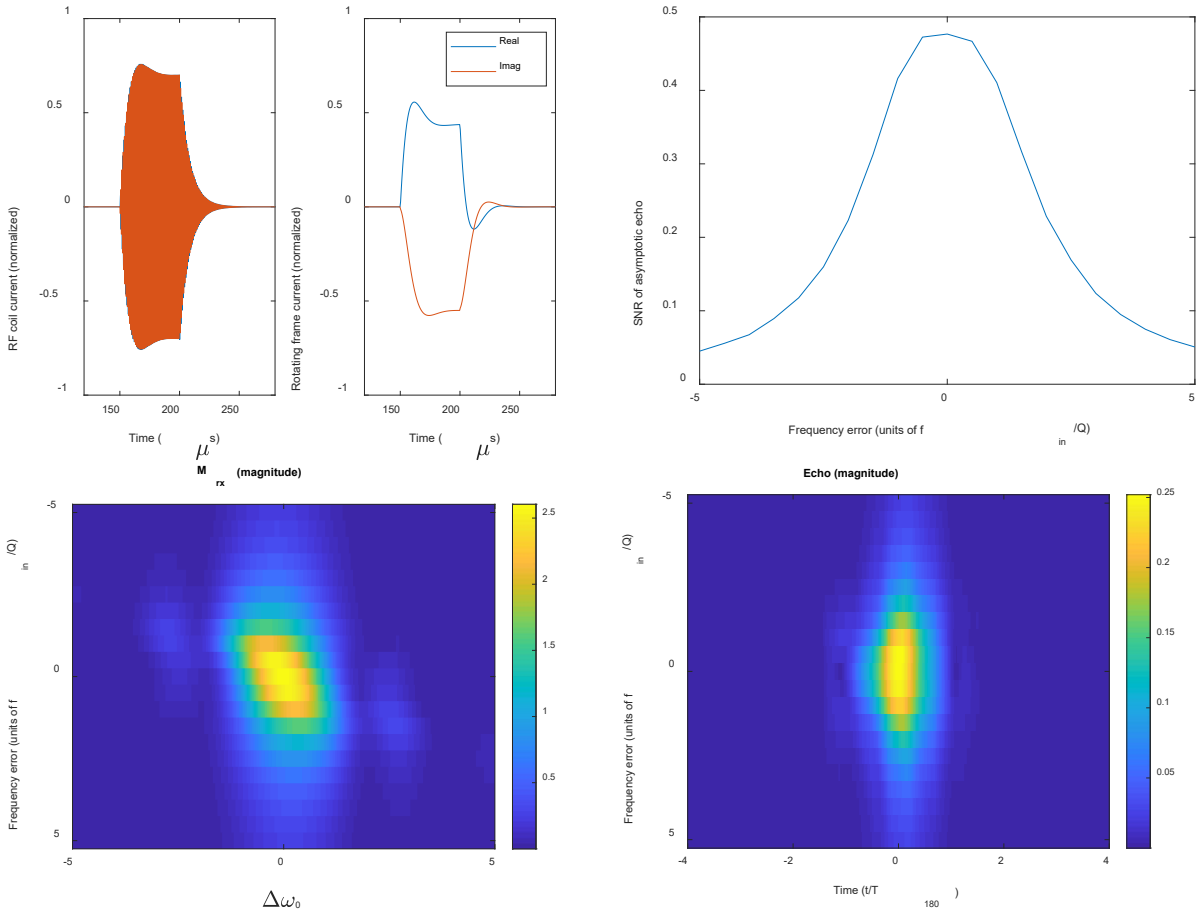

Figure 10: *CPMG pulse sequence in a uniform B_0 field gradient, with probe bandwidth effects included, as a function of probe tuning error Δf. The latter has been normalized to the nominal probe bandwidth of ~f_0/Q: (a) Refocusing pulse in the laboratory and rotating frames for $\Delta f = -1$; (b) signal-to-noise ratio (SNR) in voltage units; (c) asymptotic magnetization; and (d) asymptotic echo. The following probe and pulse sequence parameters were assumed: L = 10 μH, Q = 50, R_s = 50 Ω, f_0 = 1 MHz, T_{90} = 25 μs, $T_{180} = 2T_{90}$, $T_{acq} = 3T_{180}$.*